

PLANT SCIENCE

Biosynthesis of the allelopathic alkaloid gramine in barley by a cryptic oxidative rearrangement

Sara Leite Dias^{1†}, Ling Chuang^{2,3†}, Shenyu Liu^{2,3†}, Benedikt Seligmann², Fabian L. Brendel¹, Benjamin G. Chavez¹, Robert E. Hoffie⁴, Iris Hoffie⁴, Jochen Kümlehn⁴, Arne Bültmeier^{2,3}, Johanna Wolf², Marco Herde⁵, Claus-Peter Witte⁵, John C. D'Auria^{1*}, Jakob Franke^{2,3*}

The defensive alkaloid gramine not only protects barley and other grasses from insects but also negatively affects their palatability to ruminants. The key gene for gramine formation has remained elusive, hampering breeding initiatives. In this work, we report that a gene encoding cytochrome P450 monooxygenase CYP76M57, which we name AMI synthase (AMIS), enables the production of gramine in *Nicotiana benthamiana*, *Arabidopsis thaliana*, and *Saccharomyces cerevisiae*. We reconstituted gramine production in the gramine-free barley (*Hordeum vulgare*) variety Golden Promise and eliminated it from cultivar Tafeno by Cas-mediated gene editing. In vitro experiments unraveled that an unexpected cryptic oxidative rearrangement underlies this noncanonical conversion of an amino acid to a chain-shortened biogenic amine. The discovery of the genetic basis of gramine formation now permits tailor-made optimization of gramine-linked traits in barley by plant breeding.

Cereal crops show substantial vulnerability to biological stress because of genetic uniformity, intensive farming practices, and a lack of physical barriers such as woody tissues. Chemical defenses are therefore essential to endow grasses with protection from insects, grazing animals, and pathogens. In grasses of the family Poaceae (Gramineae), an important defensive molecule is the allelopathic indole alkaloid gramine (**1**) (Fig. 1) (1, 2). Despite its structural simplicity, gramine has a broad spectrum of activities against aphids, fungi, viruses, and other plants (3–5). It is found not only in wild grasses such as *Phalaris* spp. (6) but also in barley (*Hordeum vulgare*), the world's fourth most-widely cultivated cereal crop, according to FAOSTAT Food and Agriculture Data from the Food and Agriculture Organization of the United Nations. Although gramine confers beneficial protective properties, it can also negatively affect its usability as fodder because of its ruminant antifeedant properties (1, 5, 6). Hence, manipulating gramine levels in Poaceae through plant breeding could allow fine-tuning of the positive and negative traits associated with this alkaloid. Although gramine has been known

for more than 60 years, elucidation of the complete genetic basis of gramine biosynthesis has not been successful so far, hampering modern breeding efforts (6).

Early studies using radiolabeled precursors determined that gramine is derived from the amino acid tryptophan (**2**), with aminomethylindole (AMI) (**3**) being the key intermediate (Fig. 1) (7, 8). AMI is methylated twice by a previously described N-methyltransferase (NMT) to yield gramine via the intermediate N-methylaminomethylindole (MAMI) (**4**) (9). Labeling studies suggested that AMI retains the nitrogen of the α -amino group as well as C-3 of tryptophan, whereas C-1 and C-2 are lost (8, 10, 11). To date, neither the enzymatic basis nor the mechanism for this highly unusual rearrangement are known. It has been proposed that an enzyme that uses the cofactor pyridoxal phosphate (PLP) might carry out this reaction (fig. S1) (11, 12), but no such enzyme has yet been identified. In this work, we show that this elusive transformation is performed not by a PLP-dependent enzyme but by a cytochrome P450 monooxygenase, CYP76M57, which we name AMI synthase (AMIS). Using a combination of bioinformatics and heterologous expression, we show that the genes encoding CYP76M57 and NMT form a gene cluster in barley that correlates with the presence of gramine and are sufficient to produce gramine in *Nicotiana benthamiana*, *Arabidopsis thaliana*, baker's yeast (*Saccharomyces cerevisiae*), and a gramine-free barley cultivar. Knockout of *AMIS* in a gramine-producing barley cultivar prevented the production of gramine (**1**). In vitro experiments with yeast microsomes demonstrate how a cryptic oxidative rearrangement converts tryptophan (**1**) into AMI (**3**) via an iminium intermediate. Our results reveal the genetic and enzymatic basis of an unusual biosynthetic chain-shortening

process of an amino acid that enables further biotechnological applications of this alkaloid, which is crucial for defense in cereals.

Results

Discovery of a clustered cytochrome P450 monooxygenase gene

To initiate our search for the missing gene(s) involved in gramine biosynthesis, we analyzed the recently released pan-genome of barley that covers chromosome-scale assemblies of 20 varieties (13). Based on the previous hypothesis proposing a dependence on the cofactor PLP (fig. S1), our original intention was to select gene candidates that encode PLP-dependent enzymes. We noted a previous study that suggested the possibility of gene clustering in gramine biosynthesis (14). With this scenario in mind, we analyzed the genomic context of the previously reported *NMT* gene (9). Only one gene encoding a protein typical for specialized metabolism was found in the vicinity of *NMT*, namely a cytochrome P450 monooxygenase gene (*CYP*) at a distance of 681 kb. The cluster region also includes short sequences annotated as “transposon protein” and “nonspecific serine/threonine protein kinase” (Fig. 2A). By contrast, the closest gene encoding a PLP-dependent enzyme is located almost 5 Mb away.

Among the 20 barley lines included in the pan-genome v1 (13), six do not contain gramine (**1**) or contain only traces, whereas the others produce gramine (**1**) in the range of 700 to 6600 pmol/mg fresh weight (FW) in the leaves (15) (Fig. 2B). Genome analyses focused on *CYP* and *NMT* revealed that the presence of both genes is largely consistent with the production of gramine. All gramine-producing varieties contain both *CYP* and *NMT*, whereas Golden Promise and Morex produce neither gramine (**1**) nor AMI (**3**) and contain neither *CYP* nor *NMT*. Apparent exceptions are represented by the four accessions Du-Li Huang (ZDM_01467), Igri, Hockett, and Barke. Du-Li Huang (ZDM_01467) contains a *CYP* with a single nonconserved amino acid change [Ser²¹¹→Trp (S211W)]. Lines BIK-04-12 and HOR3081 contain other single nonconserved amino acid changes, namely Met³⁰⁰→Ile (M300I) and Met⁴⁵⁹→Ile (M459I), respectively (table S1); however, this does not seem to affect gramine production. For Igri, Hockett, and Barke, the annotated coding sequences of *CYP* are 100% identical to *CYP* from HOR10350, yet none of these varieties produce gramine. Further analysis on the genomic level revealed that the *CYP* alleles in Barke, Hockett, and Igri are all annotated to include the insertion of an intron, whereas all other accessions analyzed consist of a single exon containing the full open reading frame (fig. S2). According to the genome annotation (13), the corresponding introns include a long-terminal repeat retrotransposon (fig. S2). The

¹Department of Molecular Genetics, Leibniz Institute of Plant Genetics and Crop Plant Research (IPK), Corrensstr. 3, 06466 Seeland OT Gatersleben, Germany. ²Institute of Botany, Leibniz University Hannover, Herrenhäuser Straße 2, 30419 Hannover, Germany. ³Centre of Biomolecular Drug Research, Leibniz University Hannover, Schneiderberg 38, 30167 Hannover, Germany. ⁴Department of Physiology and Cell Biology, Leibniz Institute of Plant Genetics and Crop Plant Research (IPK), Corrensstr. 3, 06466 Seeland OT Gatersleben, Germany. ⁵Department of Molecular Nutrition and Biochemistry of Plants, Leibniz University Hannover, Herrenhäuser Straße 2, 30419 Hannover, Germany.

*Corresponding author. Email: dauria@ipk-gatersleben.de (J.C.D.); jakob.franke@botanik.uni-hannover.de (J.F.)

†These authors contributed equally to this work.

‡Present address: Department of Natural Product Biosynthesis, Max Planck Institute for Chemical Ecology, Hans-Knöll-Straße 8, 07745 Jena, Germany.

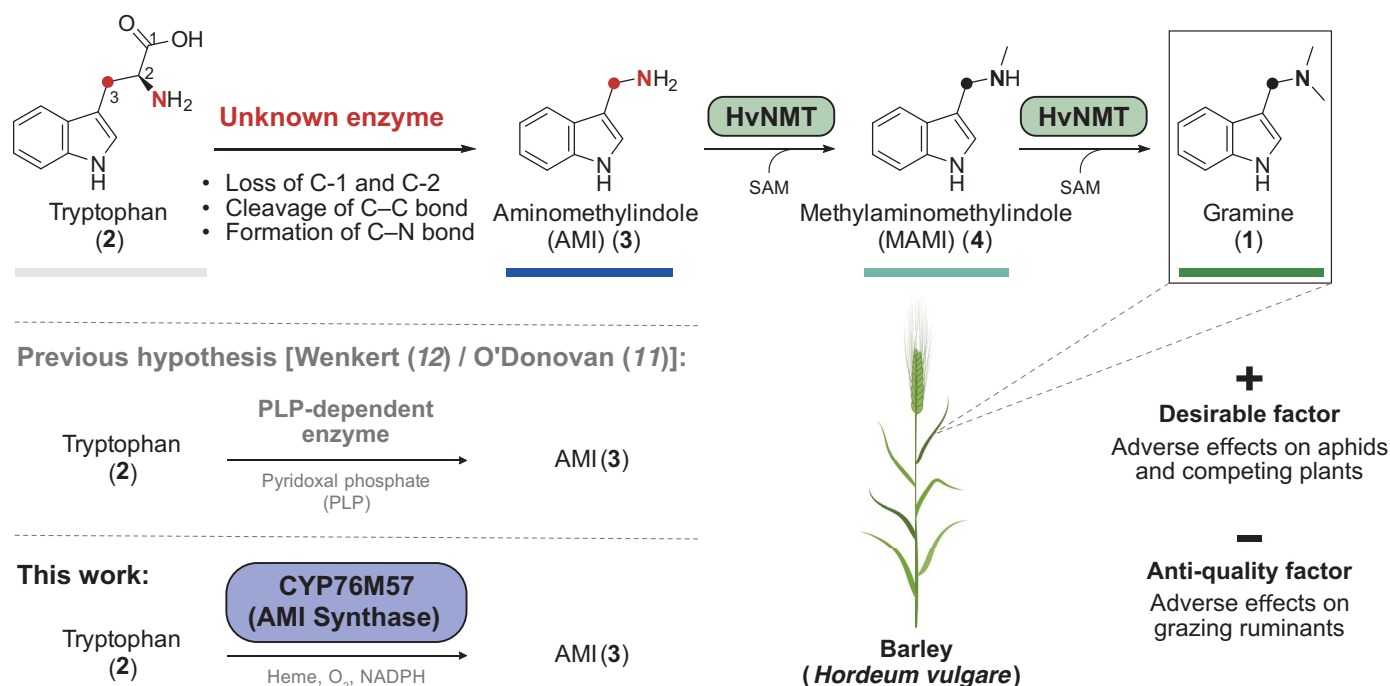


Fig. 1. Gramine (1) is a defensive alkaloid from barley (*H. vulgare*) and other Poaceae members. Gramine (1) conveys desirable as well as undesirable traits for breeding. It is derived from tryptophan (2) and produced by an uncharacterized enzyme. SAM, S-adenosyl methionine. [Part of the figure was created with BioRender.com]

presence of a transposon inside the *CYP* gene may contribute to altered expression levels because regions with these elements are often silenced (16). Taken together, this bioinformatics analysis indicated a correlation between gramine (1) production and *CYP*, suggesting that it might play a key role in gramine biosynthesis.

CYP76M57 is required for gramine biosynthesis

To test if this cytochrome P450 monooxygenase with the systematic name *CYP76M57* is involved in gramine biosynthesis, we transiently expressed *CYP76M57*, *NMT*, and a combination of both in *N. benthamiana* (17). The expression of *CYP76M57* led to the production of a new compound with a retention time, mass, and ultraviolet (UV) spectrum consistent with AMI (3) (Fig. 3A). Coexpression of *CYP76M57* and *NMT* resulted in a compound consistent with gramine (1) based on a comparison of retention time, mass, and UV spectra to a reference compound (Fig. 3A). To further corroborate the identity of heterologously produced metabolites, we isolated AMI (3) (3.2 mg/g dry weight) and gramine (1) (6.6 mg/g dry weight) and confirmed their identity by nuclear magnetic resonance (NMR) spectroscopy, a technique used for the structural characterization of organic compounds, in comparison to reference compounds (figs. S3 to S6 and tables S2 and S3). This suggested that *CYP76M57* converts tryptophan (2) into AMI (3) and consequently completes the biosynthetic pathway of gramine (1). We therefore renamed *CYP76M57* to AMI synthase (AMIS).

Our next goal was to investigate whether *AMIS* and *NMT* enable the reconstitution of gramine biosynthesis in other organisms. We chose the model plant *A. thaliana* because of the ease of the genetic transformation system that is available. After stable transformation, selected T1 plants constitutively expressing the genes *AMIS*, *NMT*, or a combination of both were tested for the presence of AMI (3) and gramine (1) by reversed-phase ultraperformance liquid chromatography fluorescence detection (RP-UPLC-FLD) (15). More than 88% ($N = 82$) of the herbicide-resistant progeny of all plants transformed with the *AMIS* construct ($N = 92$) exhibited AMI (3) concentrations above the limit of quantification. Likewise, 46% ($N = 47$) of herbicide-resistant plants transformed with the construct containing both transgenes ($N = 102$) produced gramine (1) in levels above the limit of quantification. If limits of detection are considered, 93% ($N = 86$) of the plants transformed with the *AMIS* construct produced AMI (3), and 60% ($N = 61$) of the plants transformed with the construct containing both transgenes produced gramine (1). *NMT*-transformed plants ($N = 43$), as well as control plants ($N = 16$), did not contain detectable levels of AMI (3) or gramine (1) (Fig. 3B).

To show that *AMIS* and *NMT* also enable gramine production in a nonplant organism, we integrated both genes either individually or in combination into the genome of *S. cerevisiae* (Fig. 3C). The strains further contained genes encoding *Catharanthus roseus* cytochrome P450 reductase (CPR) and cytochrome b_5 (CYB5

(18) to support cytochrome P450 monooxygenase activity. Yeast strains expressing *AMIS* produced 11.7 mg/liter of AMI (3). When both *AMIS* and *NMT* were expressed, 3.2 mg/liter of gramine (1) were produced, in addition to 3.8 mg/liter of AMI (3). Another new peak was observed in this strain, which occurred only when both *AMIS* and *NMT* were expressed. Based on a synthetic reference compound, we identified this compound as the previously reported monomethylated intermediate MAMI (4) (9), produced at a titer of 11.0 mg/liter. The total alkaloid titer of 18.0 mg/liter in the *AMIS* + *NMT* strain was slightly higher than the AMI (3) levels in the *AMIS* strain. With this yeast system, we also tested the effect of the *AMIS* mutant S211W that we noted in the barley cultivar Du-Li Huang (ZDM_01467) (Fig. 2B). Indeed, this mutation resulted in a complete loss of *AMIS* activity in yeast (fig. S7), which explains why we could not detect AMI (3) or gramine (1) in this cultivar despite the presence of the *AMIS* and *NMT* genes (Fig. 2B).

To corroborate the native role of *AMIS*, we tested it in its host plant barley (*H. vulgare*). For this, we introduced the gramine biosynthetic genes into the gramine-free variety Golden Promise and produced *AMIS* knockouts of the gramine-producing variety Tafeno. To provide the necessary genetic complementation for Golden Promise plants to produce AMI (3) and gramine (1), a construct for the integration of *HvAMIS* ("HvAMIS p6i-d35S") and one for the integration of *HvNMT* ("HvNMT p6i-d35S") were generated and used together in an

Agrobacterium-mediated cotransformation approach to transfer both constitutive expression cassettes into Golden Promise. To confirm transformation events during transgenesis, we performed polymerase chain reaction (PCR) and carried out a chemical analysis to investigate the effect of the transgenes (Fig. 3D). Thirty-seven out of the 39 transformants that exclusively carried the *AMIS* gene produced AMI (3) in amounts that averaged around 2204.05 pmol/mg FW. We also generated 10 plants that successfully integrated both *AMIS* and *NMT* and produced, on average, 40.22 pmol/mg FW of AMI (3) and 1028.77 pmol/mg FW of gramine (1).

To generate knockout plants, guide RNA (gRNA) targets based on the mRNA coding regions of *AMIS* were designed and used for targeted Cas9-mediated mutagenesis in the gramine-producing cultivar Tafeno. A vector with three specific gRNAs and a Cas9 coding sequence was built using the CasCADE sys-

tem (19), and two *Agrobacterium*-mediated transformation experiments (brh104 and brh104A) were conducted. In total, seven plants were regenerated. Genotyping revealed that five of them (brh104E1a to brh104E1c, brh104E2, and brh104AE1) were homozygous mutants ascribable to three independent mutation events, whereas two (brh104AE2 and brh104E3, respectively) were unmutated or carried heterozygous mutations and were therefore excluded from the chemical analysis reported in Fig. 3E. Homozygous deletions consisted of a 47-base pair (bp) deletion between target motifs 3 and 2 or a 34-bp deletion between target motifs 1 and 2 (see fig. S8). The 47-bp deletion creates a shift of the reading frame, resulting in a premature stop codon and a truncated protein of 44 amino acid residues. In addition to the 34-bp deletion, plant brh104AE1 also carried a biallelic 1-bp insertion at target motif 3, resulting in the alteration and deletion of a total of 16 amino acid residues (fig. S8). All transgenic plants

showed a positive signal in the *hpt*-specific PCR results. AMI (3) and gramine (1) concentrations in the plants that resulted from the three independent transformation events using the knockout construct were below limits of quantification, whereas the wild-type control plants ($N = 5$) produced an average amount of 2109.13 pmol/mg FW of gramine (1) (Fig. 3E). Altogether, the results of targeted knockout of *AMIS* in barley cv. Tafeno and the expression of *AMIS* and *NMT* in plants and yeast demonstrate that the two enzymes AMIS and NMT, possibly supported by endogenous cytochrome P450 reductases as redox partners, are sufficient to produce gramine (1).

AMIS catalyzes a rearrangement to an iminium intermediate

The process of forming AMI (3) from tryptophan (2) is mechanistically unusual because no apparent oxidation takes place that could explain the necessity of an oxidative enzyme.

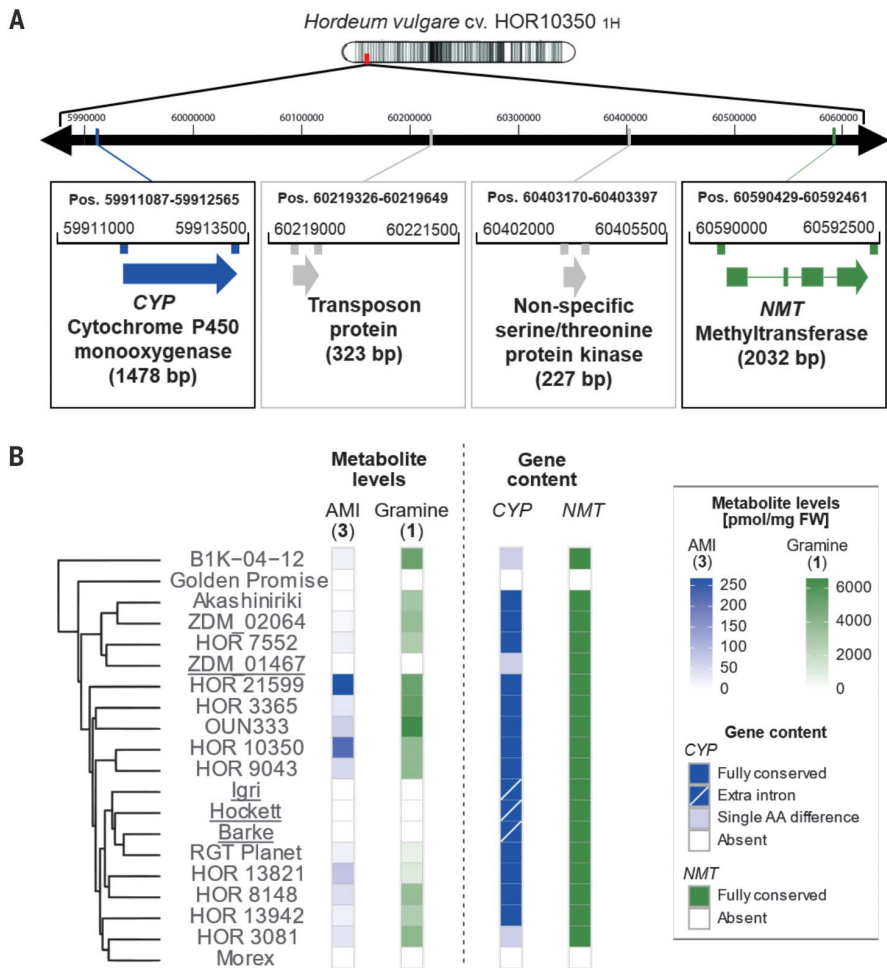


Fig. 2. The formation of gramine (1) and AMI (3) correlates with a distantly clustered cytochrome P450 monooxygenase gene in barley. (A) Loci of *CYP* (*CYP76M57*, *AMIS*) and *NMT* on chromosome 1H of *H. vulgare* cv. HOR10350. Arrow segments in zoomed-in regions indicate coding regions of exons. (B) Correlation of AMI (3) and gramine (1) levels with the *CYP* and *NMT* gene content across the 20 accessions of the barley pan-genome v1.0. The published genetic distance between accessions based on long-terminal repeat retroelements (13) is shown. Accessions with apparent mismatches (underlined) are discussed in the main text. AA, amino acid.

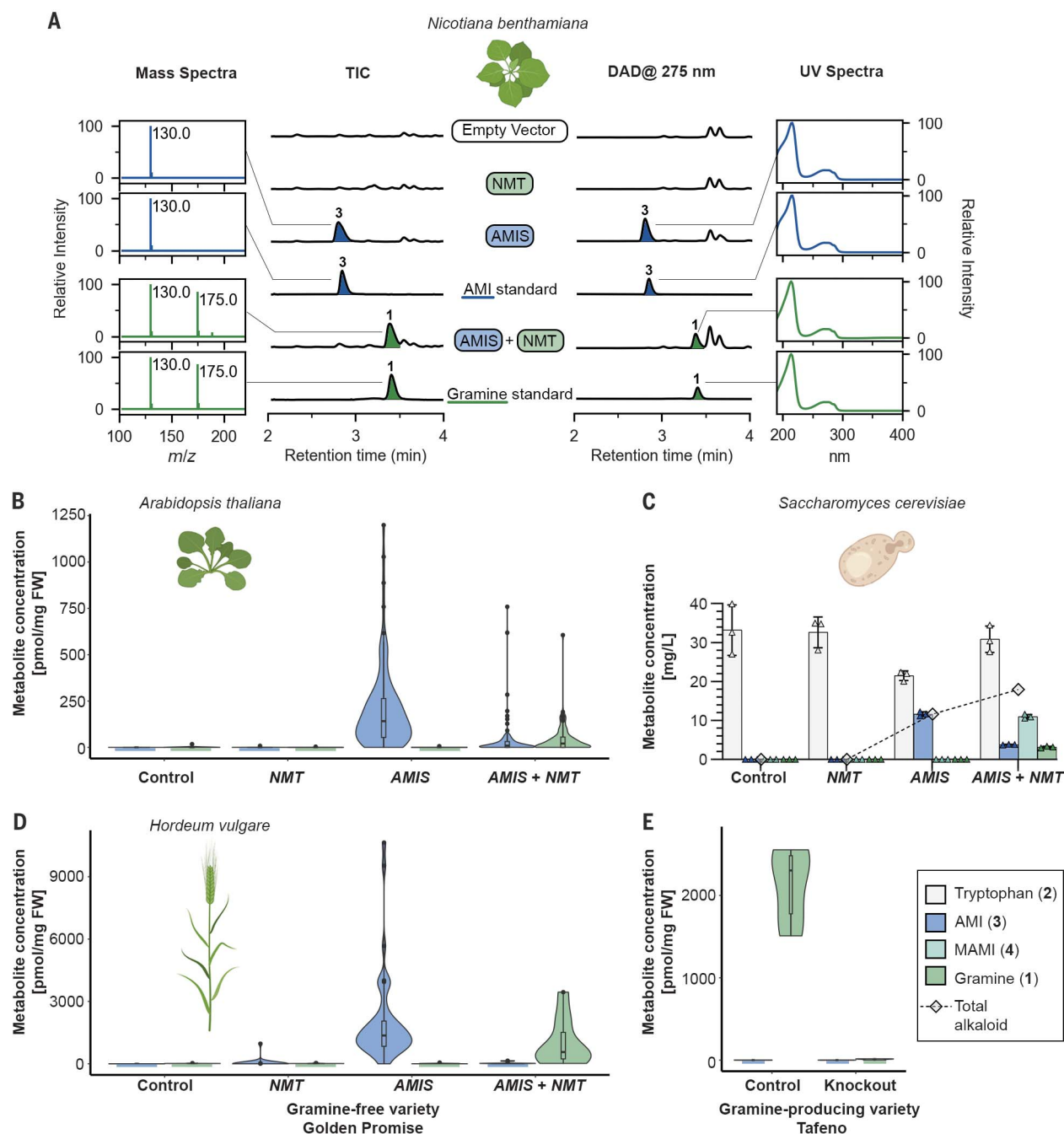


Fig. 3. AMIS (CYP76M57) and NMT are sufficient for gamine (1) biosynthesis in plants and baker's yeast. (A) Transient expression of AMIS and NMT in *N. benthamiana* leaves. DAD, diode array detector; TIC, total ion chromatogram. (B) Metabolite levels in T1 *A. thaliana* leaves stably expressing AMIS and NMT. Data are shown as violin plots for control ($N = 16$), NMT ($N = 43$), AMIS ($N = 92$), and AMIS+NMT ($N = 102$) plants. (C) Metabolite levels after genomic expression of AMIS and NMT in baker's yeast (*S. cerevisiae*). The bar plot shows means \pm SD and data points of three biological replicates. The diamond symbol indicates the total alkaloid level [AMI (3) + MAMI (4) + gamine (1)].

(D) Metabolite levels of T0 plants of *H. vulgare* cv. Golden Promise, a cultivar that does not produce gamine, transformed with AMIS and NMT. Data are shown as violin plots for control ($N = 8$), NMT ($N = 35$), AMIS ($N = 39$) and AMIS+NMT ($N = 10$) Golden Promise plants. (E) Metabolite levels of three independent transgenic *H. vulgare* cv. Tafeno plants carrying a knockout construct for AMIS. Tafeno is a gamine-producing variety. Data are shown as violin plots for control ($N = 5$) and knockout ($N = 3$) Tafeno plants. In (B), (D), and (E), boxes and whiskers represent interquartile ranges and minimum and maximum values, respectively, combined with kernel density plots. [Part of the figure was created with BioRender.com]

We therefore isolated microsomes from yeast expressing AMIS, CPR, and CYB5 to study the mechanism of AMIS. Incubation of AMIS with L-tryptophan (2) resulted in the formation of

AMI (3), whereas no AMI (3) was found in empty-vector controls (Fig. 4A). In the absence of L-tryptophan (2), small amounts of AMI (3) could be detected for microsomes containing

AMIS. We propose that this background AMI (3) was either copurified during microsomes isolation or formed by activity of AMIS with copurified L-tryptophan (2) before the start of

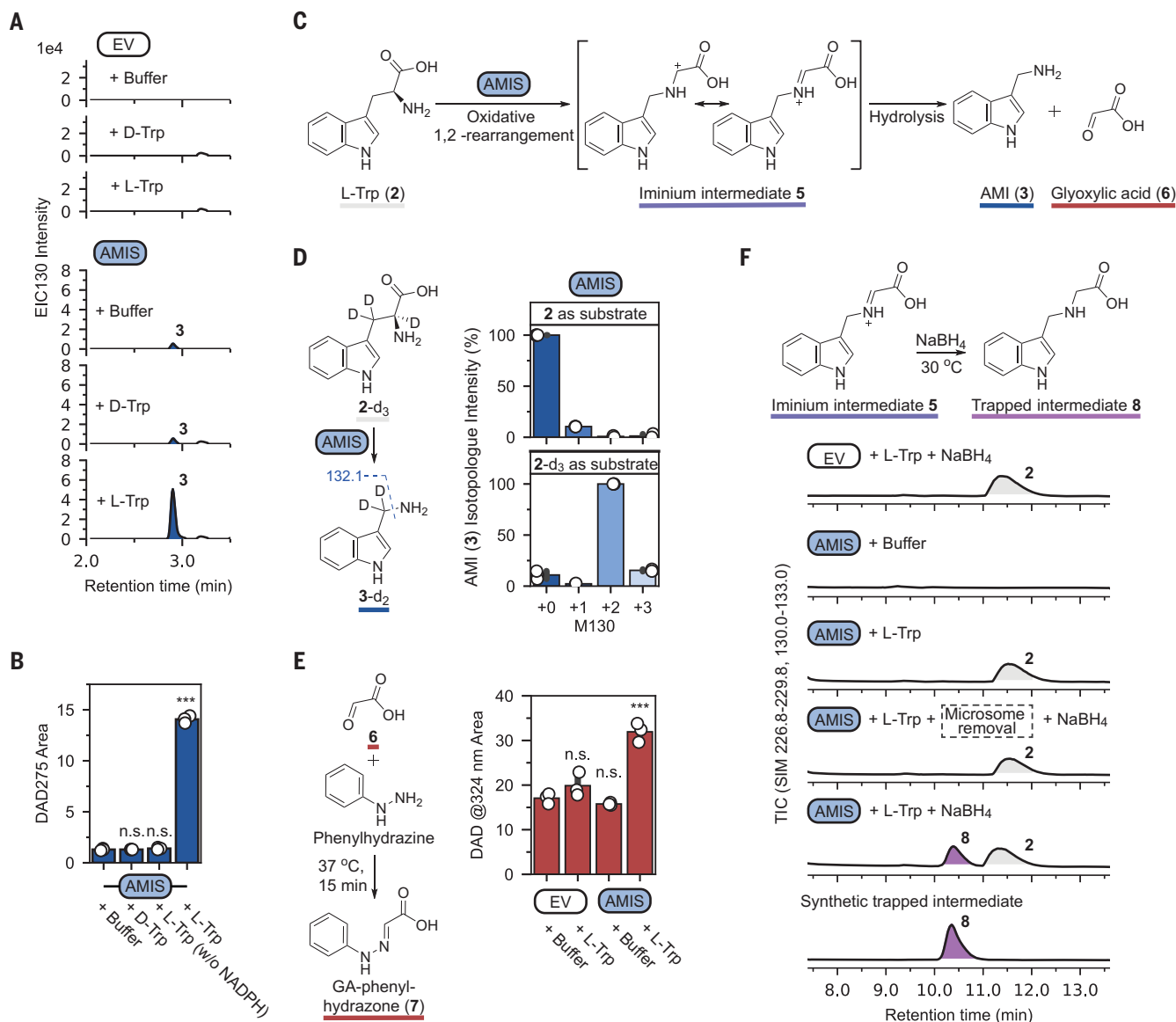


Fig. 4. AMIS catalyzes a cryptic oxidative rearrangement of L-tryptophan (2) to iminium intermediate 5 that releases AMI (3) and glyoxylic acid (6).

(A) Representative chromatograms [extracted ion chromatogram (EIC) m/z 130] of yeast microsome assays with AMIS that confirm L-tryptophan (2) as its substrate. EV, empty vector. (B) Activity of AMIS depends on L-tryptophan (2) as the substrate and NADPH. (C) Proposed mechanism for the AMIS reaction. (D) AMIS reaction with L-tryptophan-2,3,3-d₃ (2-d₃) demonstrates that no loss of deuterium label and therefore no oxidation occurs at C-3. M130 represents the in-source fragment $[M-NH_3+H]^+$ of AMI (3). (E) Glyoxylic acid (6) (GA) is

produced as a by-product from L-tryptophan (2) by AMIS. Detection was carried out after conversion to GA-phenylhydrazone (7) by high-performance liquid chromatography at 324 nm. (F) Trapping of iminium intermediate 5 with NaBH₄ from AMIS enzyme reactions with L-tryptophan (2), which results in the formation of trapped intermediate 8. The data shown are total ion chromatograms (TICs) from single-ion monitoring (SIM) mode combining m/z 227 to 230 and 130 to 133 for maximum sensitivity. All bar plots show means \pm SD and data points of three replicates. * $p < 0.05$, *** $p < 0.001$, and n.s. is not significant by Student's t test.

the assay. Assays containing D-tryptophan (99% optical purity) showed no increase in AMI (3) formation compared with those performed using controls without any substrate (Fig. 4B). We next wanted to confirm that AMIS is truly a cytochrome P450 monooxygenase. When NADPH (reduced form of nicotinamide adenine dinucleotide phosphate), the common electron donor for cytochrome P450 monooxygenases, was omitted, the activity was

indistinguishable from that of the negative control (Fig. 4B). This dependency on electron transfer was also supported in yeast; yeast strains that lacked genes for the redox partners *C. roseus* CPR and CYB5 only produced 44% of AMI (3) compared with strains that included these genes (fig. S9A). We also performed microsome assays in oxygen-depleted conditions, which was achieved by flushing the assay mixtures with nitrogen. Under these

conditions, AMI (3) production dropped to 21% compared with the positive control but could be restored to 98% by flushing the assay with pressurized air (fig. S9B). Finally, we produced a truncated and tagged soluble version of AMIS (tAMIS) in *N. benthamiana* that lacked amino acids 2 to 23 to eliminate the N-terminal membrane anchor typical of cytochrome P450 monooxygenases and that contained a hemagglutinin (HA) and StrepII

tag for affinity purification (fig. S10, A and B). Purified tAMIS contained approximately equimolar amounts of heme (fig. S10C). Taken together, our data confirm that AMIS is, despite its unusual net reaction, a canonical cytochrome P450 monooxygenase that contains heme and depends on NADPH, redox partners, and oxygen.

According to our data, AMIS catalyzes an oxidative reaction. We therefore hypothesized that the nitrogen of tryptophan is oxidized to trigger a 1,2-rearrangement of the bond between C-3 and C-2 toward the nitrogen, leading to iminium intermediate **5** (Fig. 4C). This proposal is in line with previous isotope-labeling experiments in plants that show that the nitrogen and C-3 of tryptophan (**2**) are retained in AMI (**3**), whereas C-1 and C-2 get eliminated in the form of an unknown molecular species (10). The oxidation could occur by multiple possible mechanisms (fig. S11). Hydrolysis of iminium intermediate **5** would then release AMI (**3**) as well as glyoxylic acid (**6**).

To verify this proposed mechanism, we performed enzyme assays with isotopically labeled tryptophan (**2**). Because AMI (**3**) shows complete in-source fragmentation under loss of NH_3 (10), we analyzed the isotope composition of this fragment at a mass/charge ratio (m/z) of 130. Assays carried out with tryptophan-2,3,3- d_3 (**2**- d_3) showed a clear +2 mass shift for the fragment of AMI (**3**) but no increased +1 signal (Fig. 4D). This is consistent with our hypothesis and supports the previous model (11) that no oxidation occurs at C-3.

We next wanted to confirm that glyoxylic acid (**6**) is the by-product of AMIS. We used derivatization with phenylhydrazine to phenylhydrazone adduct **7**, which is more readily detected (fig. S12) (20). Assay analysis was again complicated by a persistent background of glyoxylic acid (**6**) that was copurified during microsome preparation or produced before the assay started. Nonetheless, we detected a statistically significant increase in glyoxylic acid (**6**) levels in the presence of AMIS and tryptophan (**2**) compared with controls (Fig. 4E). We also independently quantified glyoxylic acid (**6**) levels in *N. benthamiana* after transient expression; overexpression of AMIS resulted in a significant increase in glyoxylic acid (**6**) levels in planta (fig. S13).

If AMIS oxidizes the amino group of tryptophan (**2**), *N*-hydroxy-tryptophan (**9**) could be a possible intermediate. Alternatively, *N*-hydroxy-tryptophan (**9**) might also occur as a by-product of AMIS upon premature release of an oxidized but not yet rearranged intermediate. To test these possibilities, we synthesized **9**. Although *N*-hydroxy-tryptophan (**9**) was not stable in solution, we did not observe spontaneous conversion of **9** to AMI (**3**). *N*-hydroxy-tryptophan (**9**) could also not be detected as a by-product from enzyme reactions (fig. S14). Likewise, en-

zyme assays using *N*-hydroxy-tryptophan (**9**) as a substrate did not lead to increased formation of AMI (**3**) compared with those using controls without substrate (fig. S14).

To corroborate that AMIS directly catalyzes an oxidative rearrangement, we sought to trap the proposed iminium intermediate with the reducing agent NaBH_4 , which would lead to secondary amine **8** (Fig. 4F). Assays carried out in the presence of NaBH_4 showed a new peak with a retention time and tandem mass spectrometry (MS/MS) spectrum consistent with a synthetic reference of **8** (Fig. 4F and fig. S15). This trapped intermediate **8** could not be detected when either NaBH_4 , AMIS, or tryptophan (**2**) were omitted. Also, it was not detected when NaBH_4 was added after termination of the reaction by removal of microsomal proteins, supporting that iminium intermediate **5** is a true enzymatic intermediate (Fig. 4F). When the AMIS reaction was carried out with L-tryptophan-2,3,3- d_3 (**2**- d_3) as a substrate, a +3 mass shift was observed for trapped intermediate **8**, providing further evidence that AMIS does not carry out an oxidation at C-2 or C-3 (fig. S16). Assays with L-tryptophan- $^{15}\text{N}_2$ (**2**- $^{15}\text{N}_2$) suggested that both nitrogen atoms are not separated during the reaction catalyzed by AMIS, which supports an intramolecular reaction (fig. S17). Taken together, our experiments indicate that iminium intermediate **5** is a true intermediate from the AMIS-catalyzed cryptic oxidative rearrangement of L-tryptophan (**2**).

Discussion

Although the biological relevance of gramine as a defense alkaloid in barley and other grasses is well recognized (1, 6), the genetic and enzymatic basis of its formation has remained elusive. This in turn has hindered modern molecular breeding programs that focus on sustainable pest management and sustainable agriculture. Labeling experiments led to the hypothesis that an enzyme dependent on the cofactor PLP is responsible for the formation of AMI (**3**) from tryptophan (**2**) (fig. S1) (11, 12). This would have also been in line with the canonical model of alkaloid biosynthesis, which starts with the conversion of an amino acid into a biogenic amine by a PLP-dependent decarboxylase (21). In this work, we reveal that, unexpectedly, a cryptic oxidative rearrangement plays a key role in gramine biosynthesis. A single cytochrome P450 monooxygenase, CYP76M57, which we name AMIS, converts tryptophan (**2**) into AMI (**3**) to complete the gramine biosynthetic pathway in barley. The two genes required for gramine biosynthesis form a gene cluster, which confirms the earlier hypothesis that only two colocalized genes are required for gramine biosynthesis (14). The improved availability and quality of plant genome data has accelerated the discovery of

biosynthetic gene clusters in plants (22, 23). The large intergenic distance of 681 kb between AMIS and NMT is unusual, though. It is possible that this serves a special regulatory function (24, 25). Future plant genome-mining approaches should therefore consider the possibility of distant gene clustering (22).

AMIS belongs to the CYP76 family of cytochrome P450 monooxygenases. More than 30 CYP76s from specialized plant metabolic pathways have been characterized (fig. S18), mostly from terpenoid biosynthesis (26). This includes CYP76s from the AMIS-containing subfamily CYP76M as well as from other subfamilies. Notably, CYP76M7, CYP76M8, and CYP76M14 are involved in the biosynthesis of diterpenoids such as momilactone and other phytoalexins in rice (27). Only two characterized CYP76s accept amino acid-derived substrates—CYP76AD6 and CYP76AD1 in betalain biosynthesis, which oxidize tyrosine and the related amino acid L-dopa (28). In contrast to AMIS, these enzymes act on the aromatic part of their amino acid substrate. The discovery of AMIS highlights that the substrate and reaction scope of the CYP76 family is broader than previously described and emphasizes the overall plasticity that is well known for cytochrome P450 monooxygenases in general (29, 30).

The direct rearrangement of an unmodified amino acid as catalyzed by AMIS is atypical. In the biosynthesis of glucosinolate-derived phytoalexins, superficially similar transformations occur en route to brassinin and related phytoalexins (31, 32). However, these are based on Lossen-type rearrangements of thiohydroximate-*O*-sulfonates to isothiocyanates (33) and require multiple enzymatic steps to achieve the required reactivity. Enzymatic modifications of amino acids also occur in pathways of natural products that contain nonproteinogenic α - or β -amino acids (34, 35). However, none of these enzymes performs a rearrangement like AMIS. Conceptually, the AMIS reaction resembles the Stieglitz rearrangement, which requires prior activation of the nitrogen and typically involves aromatic substituents (36). An oxidative variant of the Stieglitz rearrangement for primary amines has been reported in chemical synthesis (37). AMIS now provides a direct enzymatic connection of an amino acid to a chain-shortened biogenic amine; this reactivity enabled by an unusual cytochrome P450 monooxygenase-mediated cryptic oxidation lies outside of the scope of PLP-dependent amino acid decarboxylases, the canonical entry point into alkaloid biosynthesis (21). As such, our discovery will facilitate new avenues in synthetic biology to generate non-natural amines and alkaloids that might possess desirable biological activities.

With the description of the structural genes for gramine biosynthesis complete, it will now be possible to undertake targeted breeding

efforts aimed at modulating gramine levels or to introduce this metabolite into new host plants by incorporating its biosynthetic pathway (38). These approaches will be tailored to the myriad biological interactions in which gramine participates. Compared with many other biosynthetic pathways for metabolites of relevance to crop protection, which often require 10 or more different genes (39), gramine production is achieved by only two genes. Hence, reaching the ability to genetically engineer organisms to produce gramine seems an achievable goal.

REFERENCES AND NOTES

1. M. Vicari, D. R. Bazely, *Trends Ecol. Evol.* **8**, 137–141 (1993).
2. J. V. Lovett, A. H. C. Houlst, in *Allelopathy*, vol. 582 of ACS Symposium Series, Inderjit, K. M. M. Dakshani, F. A. Einhellig, Eds. (American Chemical Society, 1994), pp. 170–183.
3. L. J. Corcuera, *Phytochemistry* **23**, 539–541 (1984).
4. A. Lu *et al.*, *J. Agric. Food Chem.* **67**, 2148–2156 (2019).
5. K. S. Brown Jr., J. R. Trigo, in vol. 47 of *The Alkaloids: Chemistry and Pharmacology*, G. A. Cordell, Ed. (Academic Press, 1995), pp. 227–354.
6. A. D. Hanson, P. L. Traynor, K. M. Ditz, D. A. Reicosky, *Crop Sci.* **21**, 726–730 (1981).
7. E. Leete, L. Marion, *Can. J. Chem.* **31**, 1195–1202 (1953).
8. B. G. Gower, E. Leete, *J. Am. Chem. Soc.* **85**, 3683–3685 (1963).
9. K. A. E. Larsson, I. Zetterlund, G. Delp, L. M. V. Jonsson, *Phytochemistry* **67**, 2002–2008 (2006).
10. E. Ishikawa, S. Kanai, M. Sue, *Biochem. Biophys. Rep.* **34**, 101439 (2023).
11. D. O'Donovan, E. Leete, *J. Am. Chem. Soc.* **85**, 461–463 (1963).
12. E. Wenkert, *J. Am. Chem. Soc.* **84**, 98–102 (1962).
13. M. Jayakodi *et al.*, *Nature* **588**, 284–289 (2020).
14. T. J. Leland, R. Grumet, A. D. Hanson, *Plant Sci.* **42**, 77–82 (1985).
15. S. Leite Dias *et al.*, *Plants* **12**, 1930 (2023).
16. B. Liu, M. Zhao, *Curr. Opin. Plant Biol.* **75**, 102428 (2023).
17. L. Chuang, J. Franke, in *Engineering Natural Product Biosynthesis: Methods and Protocols*, vol. 2489 of Methods in Molecular Biology, E. Skellam, Ed. (Springer, 2022), pp. 395–420.
18. S. Brown, M. Clastre, V. Courdavault, S. E. O'Connor, *Proc. Natl. Acad. Sci. U.S.A.* **112**, 3205–3210 (2015).
19. I. V. O. HOFFIE, thesis, Institutionelles Repositorium der Leibniz Universität Hannover (2022).
20. M. Lange, M. Malyusz, *J. Chromatogr. B Biomed. Appl.* **662**, 97–102 (1994).
21. B. R. Lichman, *Nat. Prod. Rep.* **38**, 103–129 (2021).
22. G. Polturak, Z. Liu, A. Osbourn, *Curr. Opin. Green Sustain. Chem.* **33**, 100568 (2022).
23. S. J. Smit, B. R. Lichman, *Nat. Prod. Rep.* **39**, 1465–1482 (2022).
24. J. Colinas, S. C. Schmidler, G. Bohrer, B. Iordanov, P. N. Benfey, *PLOS ONE* **3**, e3670 (2008).
25. R. M. Clark, T. N. Wagler, P. Quijada, J. Doebley, *Nat. Genet.* **38**, 594–597 (2006).
26. U. Bathe, A. Tissier, *Phytochemistry* **161**, 149–162 (2019).
27. N. Kitaoka *et al.*, *Plant Cell* **33**, 290–305 (2021).
28. G. Polturak *et al.*, *New Phytol.* **210**, 269–283 (2016).
29. C. C. Hansen, D. R. Nelson, B. L. Møller, D. Werck-Reichhart, *Mol. Plant* **14**, 1244–1265 (2021).
30. K. Malhotra, J. Franke, *Beilstein J. Org. Chem.* **18**, 1289–1310 (2022).
31. M. S. C. Pedras, E. E. Yaya, *Org. Biomol. Chem.* **11**, 1149–1166 (2013).
32. A. P. Klein, E. S. Sattely, *Proc. Natl. Acad. Sci. U.S.A.* **114**, 1910–1915 (2017).
33. F. S. Hanschen, E. Lamy, M. Schreiner, S. Rohn, *Angew. Chem. Int. Ed.* **53**, 11430–11450 (2014).
34. F. Kudo, A. Miyanaga, T. Eguchi, *Nat. Prod. Rep.* **31**, 1056–1073 (2014).
35. J. B. Hedges, K. S. Ryan, *Chem. Rev.* **120**, 3161–3209 (2020).
36. Z. Wang, in *Comprehensive Organic Name Reactions and Reagents*, Z. Wang, Ed. (Wiley, 2010), pp. 2673–2676.
37. W. Yamakoshi, M. Arisawa, K. Murai, *Org. Lett.* **21**, 3023–3027 (2019).
38. J. Jirsitzka, D. J. Mattern, J. Gershenzon, J. C. D'Auria, *Curr. Opin. Biotechnol.* **24**, 320–328 (2013).
39. J. Zhang *et al.*, *Nature* **609**, 341–347 (2022).

ACKNOWLEDGMENTS

We thank D. Nelson (Department of Molecular Science, University of Tennessee, Memphis) and the P450 nomenclature committee for naming CYP76M57. The group of J.F. thanks S. Krause, G. Birkenbach, K. Körner, Y. Leye, and M. Fent for excellent technical and horticultural support and M. Niehaus and L. Fischer for helpful discussions. J.F. thanks C. Hertweck (Leibniz Institute for Natural Product Research and Infection Biology, HKI) and S. O'Connor (Max Planck Institute for Chemical Ecology) for helpful discussions. The group of J.C.D. thanks E. Brueckner and M. Gerres as integral members of the technical staff of the Leibniz Institute of Plant Genetics and Crop Plant Research (IPK) as well as the IPK gardener team. J.K. and R.E.H. thank S. Sommerfeld and A. Knospe for excellent technical assistance with barley transformation. The EasyClone-MarkerFree

Vector Set was a gift from I. Borodina (Addgene kit no. 1000000098). Parts of figs. S7 and S9 were created with BioRender.com. **Funding:** J.F. acknowledges financial support from the SMART BIOTECs alliance between the Technische Universität Braunschweig and the Leibniz Universität Hannover, which is supported by the Ministry of Science and Culture (MWK) of Lower Saxony. Moreover, we thank the International Max Planck Research School for supporting S.L.D. and the Leibniz Research Alliance “Bioactive Compounds and Biotechnology” for the “GraB-ME” seed-money grant to J.C.D. This work was supported by the Deutsche Forschungsgemeinschaft (DFG) INST 187/741-1 FUGG to C.-P.W. **Author contributions:** S.L.D., L.C., J.C.D., and J.F. conceived the project, designed the experiments, analyzed the data, and wrote the manuscript. S.L.D. generated the vectors for *A. thaliana* transformation, carried out the transformation, optimized the RP-UPLC-FLD method for metabolite measurement, and performed the chemical analysis of the *Arabidopsis*, Golden promise, and Tafeno plants. L.C. and J.W. performed transient expression in *N. benthamiana*. L.C. and B.S. designed and conducted enzyme assays and performed yeast microsome purifications. S.L. designed isotope-labeling experiments, synthesized and purified compounds, optimized analytical conditions, and performed NMR analysis. B.S. designed and performed the yeast metabolic engineering experiments. F.L.B. analyzed genome data. F.L.B., B.G.C., R.E.H., and I.H. generated vectors for gramine overexpression and knockout in barley. R.E.H. carried out barley transformations. J.K. designed and supervised barley transformation experiments. A.B., M.H., and C.-P.W. designed biochemical experiments. A.B. carried out biochemical experiments and heme quantification. M.H. and C.-P.W. assisted with MS/MS and high-resolution MS measurements. **Competing interests:** The authors declare that they have no competing interests. **Data and materials availability:** All data are available in the main text or the supplementary materials. The coding sequence of AMIS has been deposited in GenBank under accession number OR461264. **License information:** Copyright © 2024 the authors, some rights reserved; exclusive licensee American Association for the Advancement of Science. No claim to original US government works. <https://www.science.org/about/science-licenses-journal-article-reuse>

SUPPLEMENTARY MATERIALS

science.org/doi/10.1126/science.adk6112
Materials and Methods
Figs. S1 to S60
Tables S1 to S10
References (40–60)
MDAR Reproducibility Checklist

Submitted 7 September 2023; accepted 26 February 2024
10.1126/science.adk6112